Hindawi
Shock and Vibration
Volume 2024, Article ID 3404328, 9 pages
https://doi.org/10.1155/2024/3404328

Research Article

Research on the Influence of Characteristics of the Annular Connecting Pipe on the Transmission Loss of the Expanded Exhaust Muffler

Yue Cheng,[1] Wenhua Yuan,[1,2] Jun Fu ,[1,2] Yi Ma,[1] and Wei Zheng[3]

[1]*College of Mechanical and Engineering, Shaoyang University, Shaoyang 422000, China*
[2]*Key Laboratory of Hunan Province for Efficient Power System and Intelligent Manufacturing, Shaoyang University, Shaoyang 422000, China*
[3]*College of Intelligent Engineering, Chongqing College of Mobile Communication, Chongqing 400000, China*

Correspondence should be addressed to Jun Fu; 4160@hnsyu.edu.cn

Received 27 September 2023; Revised 10 January 2024; Accepted 16 January 2024; Published 6 February 2024

Academic Editor: Giuseppe Petrone

In order to broaden the muffler frequency band in the low-frequency range of the exhaust muffler and to achieve the purpose of broadband noise reduction, in this paper, a model of an annular connecting pipe muffler is proposed using the finite element method (FEM) to simulate the nonreflection boundary condition and to solve the transmission loss (TL). In addition, the experimental value is obtained by the spatial five-point measurement method and compared with the simulated value, and the validity and reliability of the solution model are verified. Compared with a simple expansion muffler, the average TL of the annular connecting pipe muffler is increased by 11.86 dB, and the maximum TL is increased by 18.31 dB, effectively widening the muffler frequency area, and the overall performance is effectively improved. Finally, the influence of structural factors is analyzed, including the width (W) of the annular connecting pipe, the length (L) of the annular connecting pipe, and the length ratio (m) of the front and rear chambers on the TL and on the width of the anechoic frequency band. The results reveal that the width and length of the annular connecting pipe and front-to-back cavity length ratio are the most significant factors to influence the TL, muffler frequency band, and elimination or reduction of the passing frequency, respectively.

1. Introduction

As an important part of the muffler, the resistant muffler has a good muffler effect mainly in the middle- and low-frequency range [1]. However, how to effectively improve the noise reduction performance and broaden the noise reduction frequency band has been widely considered and highly valued, and many scholars have conducted in-depth research on it [2–4]. Hou et al. [5–8] combined the flexible nozzle and the expansion muffler to propose the elastic wall expansion muffler, studying its TL. Lei et al. [9] analyzed the acoustic characteristics of the two-stage series expansion muffler. Sagar and Munjal [10] proposed an H-connected fork muffler and studied its acoustic performance. Wu and Wang [11] studied the transfer loss of a simple expansion muffler with a right-angled inlet. Fei et al. [12] used the U-shaped bellows instead of the inner intubation tube to study the muffler performance of the U-shaped bellows' band stop filter characteristics in the frequency band above the cut-off frequency of the muffler. Yasuda et al. [13] proposed a muffler with connecting holes on the tailpipe to improve the muffler performance of the tailpipe and conducted experimental and theoretical studies on the acoustic performance of the muffler in the frequency domain and time domain. Xiang et al. [14] calculated the TL of different microperforated tube lengths by using the finite element method and proposed a multicavity microperforated muffler with adjustable TL by changing the length of the third cavity. Xue et al. [15] discussed in detail the influence of geometric parameters such as the shape of the expansion chamber and

the length of the inlet and outlet on the TL. Das et al. [16] used integrated baffles in the muffler and carried out numerical simulations and experimental verification of the structure. Carbajo et al. [17] proposed a multilayer perforated plate muffler with oblique holes, predicted the acoustic performance of the multilayer perforated plate with oblique holes through the fluid equivalent theory, and carried out experimental verification on the predicted results. Zhou et al. [18] studied the low-frequency sound absorption characteristics of fixed-cavity double-layer perforated panels under the action of bias flow. The research results showed that the bias flow velocity is the key parameter that determines the sound absorption performance of the double-layer perforated panel structure. He et al. [19] found through the study of the shunt hedging anechoic unit that the anechoic performance was significantly improved after the shunt hedging. Zhang et al. [20] found through the study of the conical splitter unit that the turbulent kinetic energy of the conical splitter unit is smaller than that of the traditional anechoic unit, which can effectively suppress the generation of turbulent noise. Chang et al. [21] conducted a detailed discussion on the acoustic performance and inlet/outlet pipe parameters of a circular three-chamber muffler. Wang et al. [22] used the porous sound absorption characteristics of aerogel to explore the acoustic performance of the resonant sound absorption combination of series Helmholtz resonant mufflers. Červenka and Bednařík [23] studied the acoustic performance of mufflers with multiple ring-shaped thin expansion chambers in series with different diameters. Fu et al. [24] calculated the TL diagram of the muffler under different design parameters and analyzed the influence laws of the main parameters. Lu et al. [25] established a series-parallel coupled straight-through perforated tube muffler model, and compared it with a conventional straight-through perforated tube muffler and a straight-through double-censed perforated tube muffler, and analyzed the TL of the muffler. Chivate et al. [26] reviewed the acoustic performance of reactive silencers with simple expansion chambers. Ashok Reddy [27] conducted a literature review on acoustic research methods and materials for silencers in different fields such as automobiles, aerospace, compressors, and industrial noise.

The above studies mainly focus on improving the structure of the simple expansion muffler to improve the sound power attenuation ability at a specific frequency but did not include the expansion of the anechoic frequency band at a specific frequency. Therefore, this paper will propose an annular connected pipe muffler model based on a simple expansion muffler, aiming to study its sound power attenuation capability in the middle- and low-frequency range of 20–1200 Hz and the widening range of the muffler frequency band. The nonreflection boundary condition is mainly simulated based on the finite element method, the TL of the model is calculated, and the correctness of the model and the solution method is verified by the insertion loss (IL) test using the spatial five-point method. Finally, the influence of different structural factors on the TL is studied and analyzed.

2. Annular Connecting Pipe of the Exhaust Muffler Theory

The structural schematic diagram of the exhaust muffler of the annular connecting pipe is shown in Figure 1. When the exhaust gas enters the muffler through the inlet, it first diffuses to the first expansion chamber through the perforated pipe, and then, the sound wave propagates to the second expansion chamber through the annular connecting pipe and finally leads to the outlet through the tail perforated pipe. In this process, the change of acoustic impedance caused by the sudden change of the interface of the pipeline is used to make a part of the sound wave propagating along the pipeline reflect back to the sound source and generate a phase difference with the sound wave propagating forward, and interfere with each other, to achieve the purpose of noise reduction.

The study of sound wave propagation in pipes is the core content of acoustic calculation and analysis of mufflers. For the coaxial annular connecting pipe shown in Figure 1, the Helmholtz equation using the Laplace operator in the cylindrical coordinate system constitutes the governing equation of the sound wave propagation in the annular duct and then uses the separation of variables method to find the sound pressure analytical expression, and the radial particle vibration velocity on the rigid wall being 0 [28–30]. So, we can get the following equation:

$$J'_m(k_r a) - \left[\frac{J'_m(k_r a_1)}{Y'_m(k_r a_1)}\right] Y'_m(k_r a) = 0. \tag{1}$$

The root of the above formula can be obtained using numerical methods. For each m value, there are infinite $k_r a$ that can satisfy formula (1) and express the nth solution $k_{r,m,n}a$ with $\beta_{m,n}$. Table 1 shows the roots of formula (1), where m and n represent the circumferential and radial mode numbers.

The analytical expression of the sound pressure obtained by superimposing the sound pressure components of each mode is as follows:

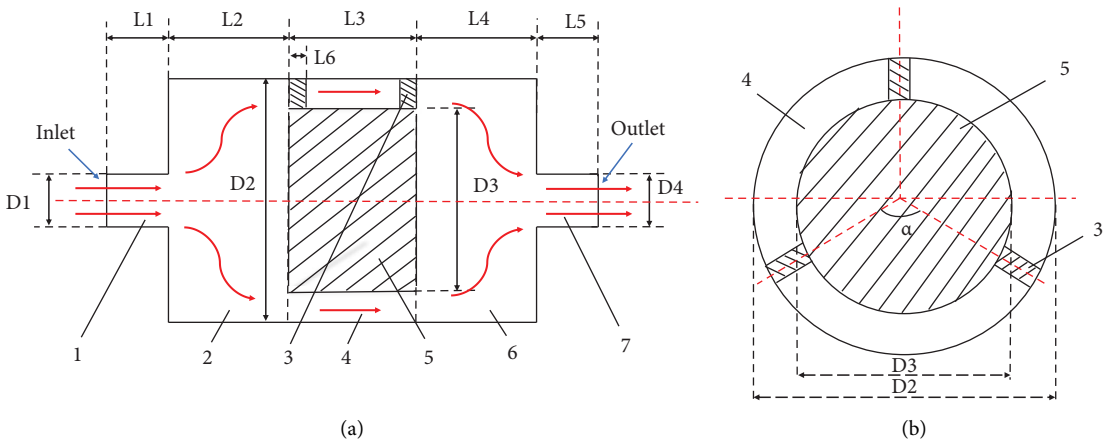

Figure 1: Structural schematic diagram of annular connecting pipe muffler. (1) Intake pipe. (2) First expansion chamber. (3) Fixed blocks. (4) Annular connecting pipe. (5) Blocking structure. (6) Second expansion chamber. (7) Exhaust pipe. (L1) Intake pipe length. (L2) First expansion chamber length. (L3) Blocking structure length. (L4) Second expansion chamber length. (L5) Exhaust pipe length. (L6) Fixed block length. (D1) Intake pipe diameter. (D2) Expansion chamber diameter. (D3) Blocking structure diameter. (D4) Exhaust pipe diameter. α-fixed block angle. (a) Sectional view of muffler front view. (b) Side sectional view of muffler.

Table 1: Solution of equation (1).

m	n					
	0	1	2	3	4	5
0	0.000	3.832	7.016	10.174	13.324	16.470
1	1.841	5.331	8.536	11.706	14.864	18.016
2	3.054	6.706	9.969	13.170	16.348	19.513
3	4.201	8.015	11.346	14.586	17.789	20.973
4	5.318	9.282	12.682	15.964	19.196	22.401
5	6.415	10.520	13.987	17.313	20.576	23.804

$$
\begin{aligned}
p_{(r,\theta,z)} = {} & \sum_{n=0}^{\infty} R_0\left(\beta_{(0,n)}\frac{r}{a}\right)\left\{A_{(0,n)}[ee]^{-jk_{z,0,n^z}} + B_{(0,n)}[ee]^{jk_{z,0,n^z}}\right\} \\
& + \sum_{m=1}^{\infty}\sum_{n=0}^{\infty} R_m\left(\beta_{(m,n)}\frac{r}{a}\right)\left\{\left[A^{+}_{(m,n)}[ee]^{-jm\theta} + A^{-}_{(m,n)}[ee]^{jm\theta}\right][ee]^{-ik_{z,m,n^z}}\right. \\
& \left. + \left[B^{+}_{(m,n)}[ee]^{-jm\theta} + B^{-}_{(m,n)}[ee]^{jm\theta}\right][ee]^{jk_{z,m,n^z}}\right\},
\end{aligned}
\tag{2}
$$

where $R_m(\beta_{(m,n)}r/a) = J_m(\beta_{(m,n)}r/a) - [J'_m\beta_{(m,n)}/Y'_m\beta_{(m,n)}]Y_m(\beta_{(m,n)}r/a)$. Also, the axial wave number $(k_{z,m,n})$ of the (m, n) mode is determined by the following formula:

$$
k_{z,m,n} = \left[k^2 - \left(\frac{\beta_{m,n}}{a}\right)^2\right]^{1/2}. \tag{3}
$$

The first circumferential mode starts to propagate at $ka = \beta_{1,0}$, and the first radial mode starts to propagate at $Ka = \beta_{0,1}$, so the plane wave cut-off frequency is

$$
f_{\text{cut-off}} = \frac{\beta_{1,0}}{2\pi a}C. \tag{4}
$$

Since the inlet and outlet boundary conditions of the model in this paper are axisymmetric, the first higher-order mode is the radial mode at this time, and its plane wave cut-off frequency is

$$
f_{\text{cut-off}} = \frac{\beta_{0,1}}{2\pi a}C, \tag{5}
$$

where the speed of sound at $C = 340$ m/s, a (0.17 m) is the radius of the circular duct, and $\beta_{0,1}$ is 3.832. From this, it can be calculated that the plane wave cut-off frequency of the ring muffler is 1219.76 Hz.

3. Structural Dimension Design

The specific structure of the exhaust muffler of the annular connecting pipe is shown in Figure 1, and the structural dimensions are shown in Table 2. Annular connecting pipe exhaust muffler includes intake pipe-1, first expansion chamber-2, fixed blocks-3, annular connecting pipe-4, blocking structure-5, second expansion chamber-6, and exhaust pipe-7.

Table 2: Annular connecting pipe exhausts muffler structure size.

Part	L1 (mm)	L2 (mm)	L3 (mm)	L4 (mm)	L5 (mm)	L6 (mm)	D1 (mm)	D2 (mm)	D3 (mm)	D4 (mm)	α (°)
Size	50	99	102	99	50	10	52	340	320	52	120

The exhaust muffler of the annular connecting pipe fixes the blocking structure in the expansion chamber of the ordinary single expansion muffler through the fixing block, and then divides the single expansion chamber into front and rear double chambers, and forms an annular connecting pipe. In the simulation calculation, the parameters such as the diameter-D3, length-L3, and length ratio of the front and back cavity-m (L2/L4) of the blocking structure are changed in sequence, and the influence of each parameter is changed on the TL.

4. Acoustic Performance Analysis

4.1. Boundary Condition Settings. Making Assumptions during Acoustic Simulation Calculations. The wall boundary is a rigid wall, ignoring the sound absorption of the wall.

Define Acoustic Domain Materials and Properties. Due to the low influence of the components in the automobile exhaust on the acoustic performance and to simplify the calculation process and the difficulty of material definition, the internal fluid material can be approximately defined as air in the acoustic simulation, the density of the fluid, and the velocity of sound can then be determined.

The upper limit cut-off frequency of the exhaust muffler of the annular connecting pipe is 1219.76Hz, and the lower limit frequency that the human ear can hear is 20Hz. Therefore, 20 Hz–1220 Hz is taken as the main research frequency range of this paper.

In the simulation process, the mesh type adopts free tetrahedral mesh, the acoustic grid size (λ) should meet the requirements of formula (6), and the calculation formula is

$$\lambda \leq \frac{C}{6f_{\max}}, \tag{6}$$

where λ is the acoustic grid size (m); C is the speed of sound in air (m/s), $C = 340$ m/s; $f_{\max}$ is the highest frequency for acoustic calculations.

Since the calculation frequency range is low-medium frequency (20 Hz–1200 Hz), $f_{\max}$ chooses 1200 Hz; by substituting C and $f$max into the calculation formula, we can get $\lambda = 0.0472$ m; this paper defines the maximum grid size as 0.01 m, and the minimum grid size is defined as 0.005 m, smaller than the calculated acoustic mesh size and meet the requirements.

TL is defined as the difference between the incident sound power level at the inlet of the muffler and the transmitted sound power level at the outlet [31]. Its calculation formula is as follows:

$$\mathrm{TL} = L_i - L_t = 10\,lg\left(\frac{W_i}{W_t}\right), \tag{7}$$

where W_i and W_t are the incident sound power at the inlet and the transmitted sound power at the outlet of the muffler.

The boundary condition of the inlet and outlet of the muffler is defined as follows: (1) the inlet of the annular connecting pipe exhaust muffler is defined as a circular port and the incident wave power is 1W and (2) the outlet of the annular connecting pipe exhaust muffler is defined as a circular port and with no reflection boundary condition.

4.2. Transmission Loss Analysis. Using the FEM, the TL of the exhaust muffler in the 20 Hz–1200 Hz range was obtained through simulation calculations. It was then compared with a simple expansion muffler to generate a TL comparison graph, as shown in Figure 2.

Through the simulation analysis results, it can be seen that the TL of the simple expansion muffler in the range of 20 Hz–1200 Hz exhibits periodic oscillation under the condition of the same shape and volume of the two mufflers. There will be a failure frequency every 550 Hz–600 Hz intervals, the maximum TL is 18.1 dB, and the average TL is 13.09 dB. Compared with the simple expansion muffler, the muffler with an annular connecting pipe only has one failure frequency in the range of 20–1200, the noise reduction frequency band is wider, the maximum TL is 36.23 dB, and the average TL is 24.95 dB.

In the low-frequency range I (20 Hz–210 Hz), the annular connecting pipe muffler has lower TL, and there is a failure frequency at 210 Hz; the main reason is that in the 20 Hz–210 Hz frequency range, low-frequency resonance noise will be generated inside the muffler, resulting in low noise reduction performance in this area. In the medium-frequency range II (210 Hz–1200 Hz), the TL of the annular connecting pipe muffler is higher than that of the simple expansion muffler at all frequencies, and the maximum TL difference is 18.2 dB.

5. Annular Connecting Pipe Muffler Test

5.1. Test Equipment. The built test bench is shown in Figure 3. It mainly includes 192 series air-cooled diesel engine, eddy current dynamometer, FC2000 diesel engine measurement and control system, HS5670B average sound level meter, tripod head, acoustic panels, annular connecting pipe muffler, and computer.

5.2. Test Principle and Data Collection. TL and IL can reflect the acoustic performance of the muffler from different aspects, but the measurement of TL requires specialized equipment and is expensive, and IL is much easier to measure than TL [32, 33]. Therefore, this paper uses the spatial five-point measurement method to measure the IL of

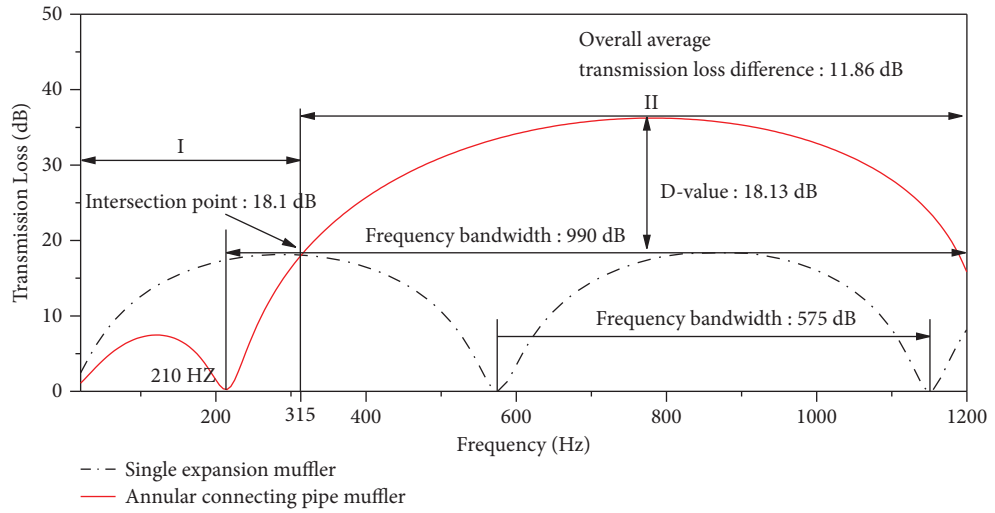

Figure 2: Transmission loss comparison chart.

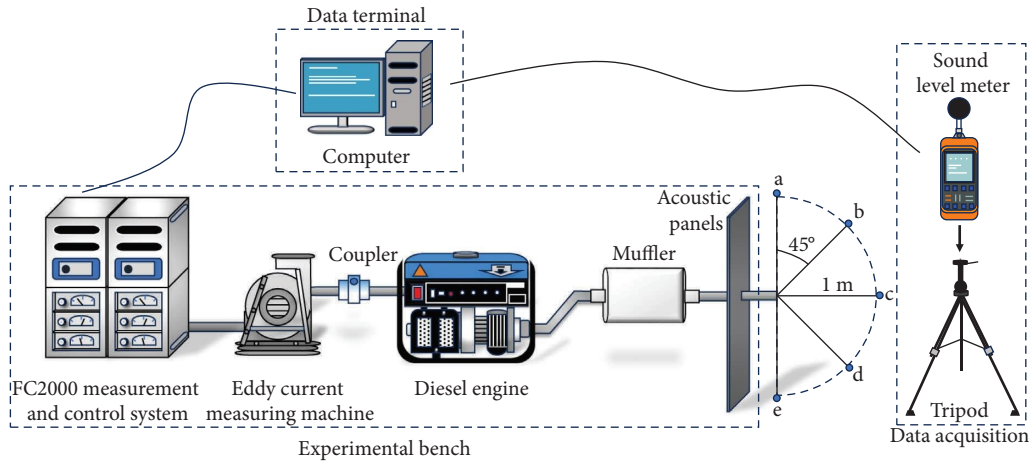

Figure 3: Schematic diagram of the test bench.

the muffler. Finally, the TL is approximately calculated by the conversion formula (8) of sound power level and sound pressure level.

$$\begin{cases} \mathrm{TL} = L_{W_1} - L_{W_2}, \\ \mathrm{IL} = L_{P1} - L_{P2}, \\ L_W = L_P + 20\lg r + 11, \end{cases} \tag{8}$$

where r is the distance from the tail end of the exhaust pipe to the test point ($r = 1$ m in this paper), L_{P1} and L_{P2} are the sound pressure levels before and after the muffler is installed, and L_{w_1} and L_{w_2} are the sound power levels at the entrance and exit, respectively.

In this paper, the IL is measured by the spatial five-point measurement method, as shown in Figure 3. We take the center of the exhaust pipe outlet end face as the reference point, take the plane where the exhaust pipe outlet end face is located as the reference plane, select two measurement points 1m away from the reference point on the reference plane (point a and point e), then select a measurement point every 45° between point a and point e (point b, point c, and point d), and, at the same time, ensure that the distance between the five measurement points and the ground is 1 m. When the diesel engine is running, we select the normal working condition with a speed of 1800 r/min and a load of 75%. During the test, three repeated acquisitions were performed at each acquisition frequency, and all were recorded; it is considered reliable data when the deviation of three readings is less than 0.5 dB, and after completing the data collection and processing, the approximate conversion of the TL is carried out according to formula (8).

5.3. Data Analysis. For the annular connecting pipe muffler, in this paper, the simulation value of TL is obtained by FEM, to verify the reliability of the simulation method and model, the IL is obtained through experiments, and then, the TL is obtained through the transformation of the formula (8). Comparing the simulated value with the experimental value, a comparison chart is obtained, as shown in Figure 4.

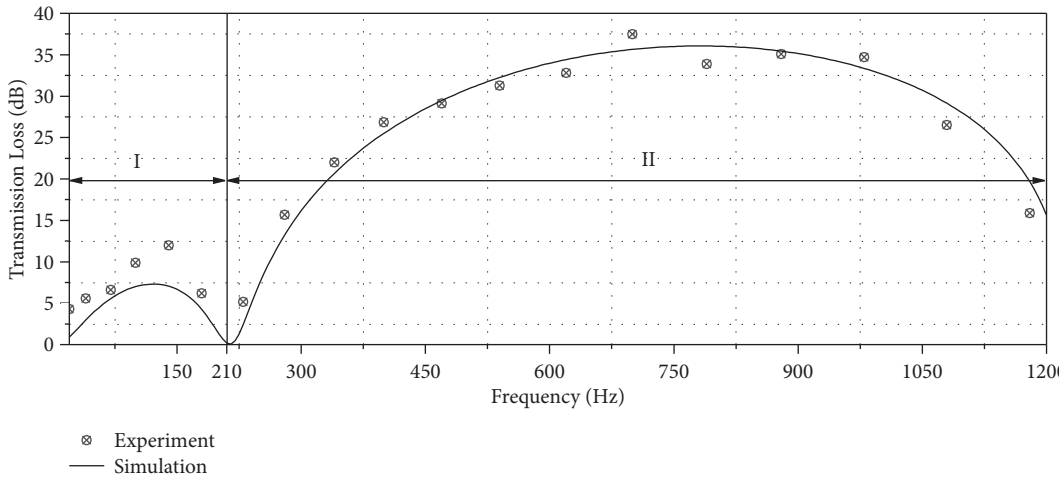

Figure 4: Comparison chart of TL experiment and simulation.

It can be seen from Figure 4 that in the frequency range II (20 Hz–210 Hz), the experimental values are higher than the simulated values because resonance noise generated by air resonance may occur in the low-frequency range. In the frequency range II (210 Hz–1200 Hz), the difference between the experimental value and the simulated value is small. Through calculation, the error between the experimental value and the simulation value is 3.31%, and the reason may be as follows: (1) there is air resonance in the low-frequency range, which produces resonance noise, (2) ambient noise may influence the measured values, (3) effect of engine exhaust temperature and aerodynamic performance on exhaust noise, and (4) TL is obtained through formula conversion.

6. Influence Law of Structural Factors

The main structural parameters affecting the exhaust muffler of the annular connecting pipe are the width and length of the annular connecting pipe. Therefore, the research on the influence law of the structural factors of the annular connecting pipe mainly considers its width, length, and front-to-back cavity ratio. Due to the previous acoustic analysis, the upper and lower limit cut-off frequency range of the muffler is 21.37 Hz–1220 Hz, it has good reference value in this range, and, at the same time, the boundary condition parameters required by the structural scheme are the same as those set above.

6.1. Analysis of the Influence of Annular Connecting Pipe Width on TL. Changing the W (W = (D2-D3)/2) of the annular connecting pipe of the muffler to 5 mm, 10 mm, 15 mm, 20 mm, and 40 mm, the rest of the structural dimensions are consistent with those shown in Table 2. The simulation results are shown in Figure 5.

From Figure 5, it can be found that the smaller the width W of the annular connecting pipe in the middle- and low-frequency range of 20 Hz–1200 Hz, the higher the peak value of TL, the wider the frequency band of TL, and the number of zero points decreases, when W is between 5 mm and 40 mm, the maximum peak difference of TL is close to 17 dB, and the average TL is increased by 12.71 dB. In the frequency range I (20 Hz–500 Hz), the first zero point appears on the TL curve, but with the decrease of W, the TL zero point gradually moves to low frequency, and the first peak gradually decreases; in the frequency range II (500 Hz–1100 Hz), the overall TL presents a broadband noise reduction trend, as the width W gradually decreases, the peak value of the TL gradually increases, and the curvature of the TL curve gradually decreases; in the frequency range III (1100 Hz–1200 Hz), the second zero point appears, but as W decreases, the zero point position gradually moves to the right, and the slope of the tangent line of the TL curve becomes smaller.

On the whole, W has a great influence on the TL, which is mainly reflected in the influence on the position of two zero points (anechoic bandwidth), the peak value of the TL and the average value of the TL. Additionally, it should be noted that the change in w only changes the position of the zero point but does not alter the trend of the TL curve.

6.2. Analysis of the Influence of Annular Connecting Pipe Length on TL. Changing the L3 of the annular connecting pipe of the muffler (62 mm, 82 mm, 102 mm, 122 mm, and 162 mm), the rest of the structural dimensions are consistent with those shown in Table 2. The simulation results are shown in Figure 6.

From the TL curve in Figure 6, it can be seen that the TL changes with the change of L3, and the smaller the L3, the wider the TL frequency band. In the frequency range I (20 Hz–330 Hz), the first zero point appears on the TL curve, and with the gradual increase of L3, the zero-point position gradually moves to the low frequency, and, at the same time, the peak value in this region gradually decreases. In the frequency range II (330 Hz–920 Hz), the overall TL shows the trend of broadband noise reduction, and with the increase of L3, the peak gradually moves to the high-frequency direction. In the frequency range (920 Hz–1200 Hz), with the gradual decrease of L3, the second zero point appears in

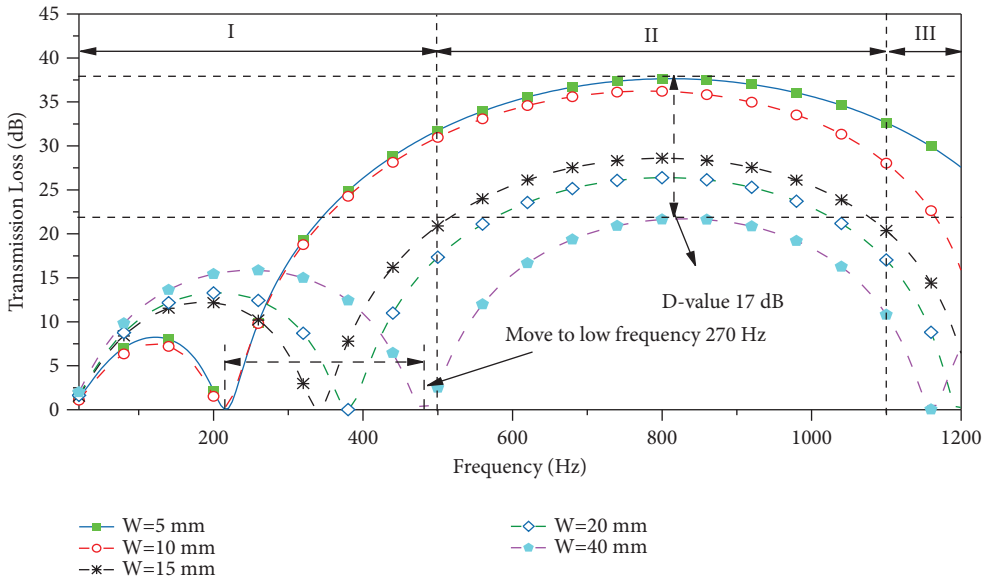

Figure 5: TL curves of annular connecting pipes with different widths.

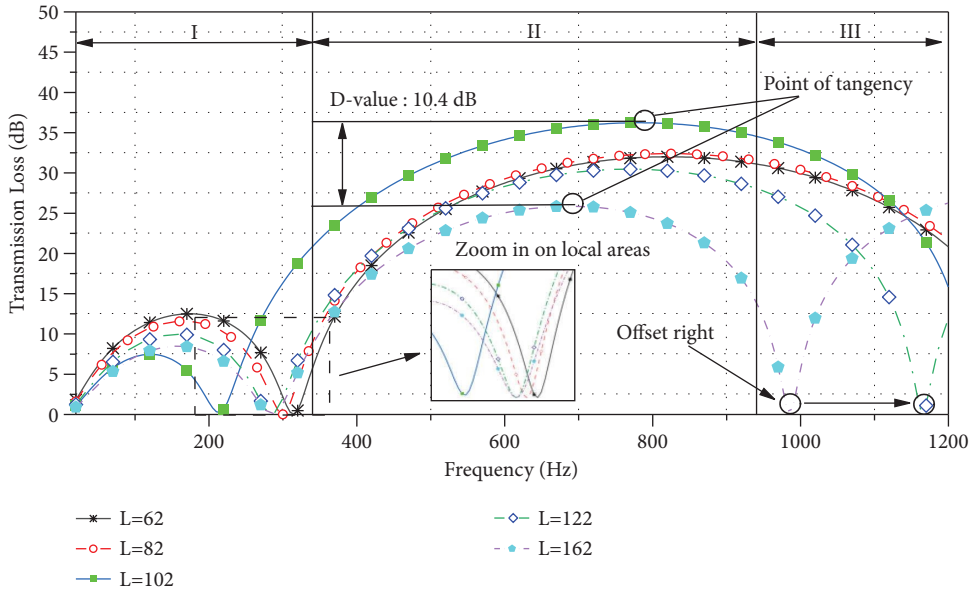

Figure 6: TL curves of annular connecting pipes with different lengths.

turn and the zero-point position gradually moves to high frequency. Overall, L3 has a greater impact on the bandwidth of the transmission loss anechoic frequency.

6.3. Analysis of the Effect of the Length Ratio of the Front and Back Cavity on the TL. Changing the length ratio of the front and rear chambers of the annular connecting pipe muffler m ($m = L2/L4$) to 1 : 1 (99 : 99), 1 : 1.5 (79.2 : 118.8), 1 : 2 (66 : 132), 1 : 2.3 (60 : 138), 2.3 : 1 (138 : 60), the rest of the structural dimensions are consistent with those shown in Table 2. The simulation results are shown in Figure 7.

From Figure 7, it can be found that the TL changes with the change of m in the frequency range of 20 Hz–1200 Hz, and the anechoic frequency band of the TL is wider with the increase of m. In the frequency range I (20 Hz–320 Hz), the first trough appears in the transmission loss curve. When $m = 1$, the TL curve appears at zero point (TL = 0), but with the gradual decrease of m, the zero point disappears, and the TL gradually increases at the trough position. In the frequency range II (320 Hz–1140 Hz), the anechoic frequency band is wider, and the average TL increases with the increase of m. In the frequency range III (1140 Hz–1200 Hz), there is a second trough in the TL curve but no zero point, and the position of the second trough gradually moves to the high-frequency direction with the increase of m; in addition, it is also found that the TL curves of the front-to-back cavity length ratio of 1 : 2.3 and 2.3 : 1 coincide, and it can be seen that when m is the reciprocal of each other, the TL is the same.

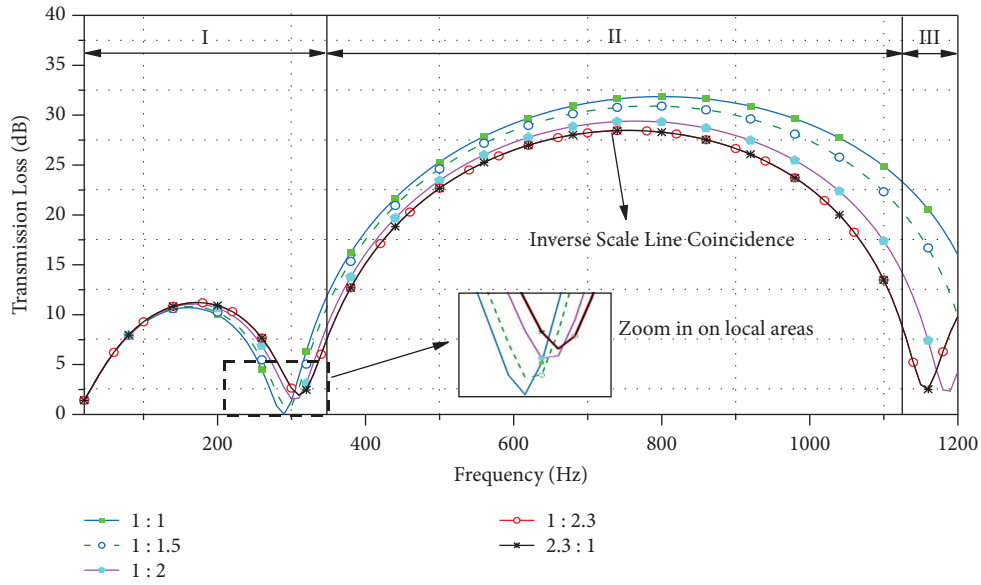

Figure 7: TL curves of different front and rear chamber length ratios.

Overall, the influence of m on the TL in the range of 20 Hz–1200 Hz is relatively small. As m is closer to 1, the anechoic frequency band is wider, and when $m \neq 1$, the TL zero point disappears; the main reason is that when $m = 1$, the front and rear chambers have the same anechoic frequency (pass frequency same), and when $m \neq 1$, the anechoic frequencies of the front and rear chambers are different, and the passing frequency disappears, so the zero point of TL disappears.

7. Conclusions

This paper proposes an annular connecting pipe exhaust muffler. The simulation value of the TL is obtained through the FEM, and the test value is obtained by using the space five-point measurement method and the diesel engine test bench, and the reliability of the simulation model and method is verified by comparing the simulation value with the test value. In addition, the simulation analysis of the influence of structural factors (annular connecting pipe width, annular connecting pipe length, and the length ratio of the front and rear cavity of the annular connecting pipe muffler) on the transmission loss of the muffler was carried out, and the following conclusions were obtained:

(1) In the frequency range of 20 Hz–1200 Hz, compared with the simple expansion muffler, the average TL of the annular connecting pipe muffler is increased by 11.86 dB, and the peak value of the TL is increased by 18.31 dB, effectively broadening the noise reduction frequency band, and the overall noise reduction performance has been significantly improved.

(2) Changing the width of the annular connecting pipe has a great influence on the average TL, the peak value of the TL, and widening the noise reduction frequency band.

(3) Changing the length of the annular connecting pipe has little effect on the peak value of the muffler's TL but has a greater effect on widening the noise reduction frequency band.

(4) Changing the length ratio of the front and rear cavities has little effect on the TL value of the muffler but has a certain influence on the width of the muffler frequency band. When the length of the front and rear cavities is different, the pass frequency can be eliminated.

(5) When considering the influence of muffler structural factors on muffler performance indicators, for the transmission loss value, the influence of the width of the ring connection pipe should be given priority, and for the width of the noise reduction frequency band, the influence of the length of the annular connecting pipe should be given priority, and for the elimination or reduction of the passing frequency, the effect of the front-to-back cavity length ratio should be given priority.

Data Availability

The data used to support the findings of this study are available from the corresponding author upon request.

Conflicts of Interest

The authors declare that they have no conflicts of interest.

Acknowledgments

This work was supported by the National Natural Science Foundation of China (Grant no. 52076141), Hunan Provincial Natural Science Foundation of China (Grant no. 2022JJ50025), Hunan Provincial Natural Science Foundation of China (Grant no. 2023JJ50262), Postgraduate

Scientific Research Innovation Project of Hunan Province (Grant no. CX20221309), and Shaoyang University Innovation Foundation for Postgraduate (Grant no. CX2022SY001).

References

[1] Y. L. Shao, "A study on exhaust muffler using a mixture of counter-phase counteract and split-gas rushing," *Procedia Engineering*, vol. 15, pp. 4409–4413, 2011.

[2] T. Yasuda, C. Wu, N. Nakagawa, and K. Nagamura, "Predictions and experimental studies of the tail pipe noise of an automotive muffler using a one dimensional cfd model," *Applied Acoustics*, vol. 71, no. 8, pp. 701–707, 2010.

[3] S. Quanquan, Y. Yuzhen, Z. Zhun, A. Bingwen, T. Pengyi, and J. Chengcheng, "Research and design of broadband muffler based on second-order Helmholtz resonators," *Acta Physica*, vol. 71, no. 23, pp. 302–310, 2022.

[4] G. Montenegro, A. Onorati, and A. Della torre, "The prediction of silencer acoustical performances by 1d, 1d–3d and quasi-3d non-linear approaches," *Computers & Fluids*, vol. 71, pp. 208–223, 2013.

[5] H. Jiuxiao, Z. Haichao, M. Rongfu, and Y. Suwei, "Transmission loss characteristics of expansion muffler with flexible walls," *Journal of Ship Mechanics*, vol. 25, no. 4, pp. 517–525, 2021.

[6] H. Jiuxiao, Z. Haichao, Y. Suwei, and L. Jinlong, "Low-frequency broadband characteristics of a plate silencer with a flexible back cavity," *Journal of Vibration and Shock*, vol. 39, no. 20, pp. 251–257, 2020.

[7] Y. Suwei, Z. Haichao, and H. Jiuxiao, "Finite element analysis of perforated tube water muffler with flexible dorsal cavity," *Ship Science and Technology*, vol. 43, no. 3, pp. 76–79, 2021.

[8] H. Jiuxiao, Z. Haichao, M. Rongfu, and Y. Suwei, "Acoustic characteristic of drum-like silencer with flexible back cavity," *Journal of National University of Defense Technology*, vol. 41, no. 6, pp. 75–82, 2019.

[9] H. Lei, J. Hongli, Q. Jinhao, and W. Yipeng, "Analysis of acoustic characteristic of expansion muffler in two stage series," *Chinese Journal of Applied Mechanics*, vol. 35, no. 1, pp. 60–64, 2018.

[10] V. Sagar and M. Munjal, "Analysis and design guidelines for fork muffler with H-connection," *Applied Acoustics*, vol. 125, pp. 49–58, 2017.

[11] C. Wu and C. Wang, "Attenuation for the simple expansion chamber muffler with a right angle inlet," *Journal of Mechanics*, vol. 27, no. 3, pp. 287–292, 2011.

[12] X. Fei, S. Beibei, and C. Jiandong, "A study on the feasibility of the application of the U-shaped corrugated Pipes in reactive mufflers," *Journal of Vibration and Shock*, vol. 37, no. 20, pp. 230–236, 2018.

[13] T. Yasuda, C. Wu, N. Nakagawa, and K. Nagamura, "Studies on an automobile muffler with the acoustic characteristic of low-pass filter and Helmholtz resonator," *Applied Acoustics*, vol. 74, no. 1, pp. 49–57, 2013.

[14] L. Xiang, S. Zuo, X. Wu, and J. Liu, "Study of multi-chamber micro-perforated muffler with adjustable transmission loss," *Applied Acoustics*, vol. 122, pp. 35–40, 2017.

[15] Y. Xue, G. Jin, T. Ye, K. Shi, S. Zhong, and C. Yang, "Isogeometric analysis for geometric modelling and acoustic attenuation performances of reactive mufflers," *Computers & Mathematics with Applications*, vol. 79, no. 12, pp. 3447–3461, 2020.

[16] S. Das, S. Das, K. Mondal Das et al., "A novel design for muffler chambers by incorporating baffle plate," *Applied Acoustics*, vol. 197, Article ID 108888, 2022.

[17] J. Carbajo, S. Ghaffari mosanenzadeh, S. Kim, and N. Fang, "Multi-layer perforated panel absorbers with oblique perforations," *Applied Acoustics*, vol. 169, Article ID 107496, 2020.

[18] H. Zhou, S. Meng, C. Tao, and Z. Liu, "Low-frequency sound absorptive properties of dual perforated plates under bias flow," *Applied Acoustics*, vol. 146, pp. 420–428, 2019.

[19] S. He, W. Pei, Z. Yongan, X. Jing, and Z. Haijun, "Analysis on the flow field characteristics of the split-stream rushing exhaust muffler for diesel engine," *Journal of Inner Mongolia Agricultural University (Natural Science Edition)*, vol. 42, no. 1, pp. 68–72, 2021.

[20] Y. Zhang, P. Wu, Y. Ma, H. Su, and J. Xue, "Analysis on acoustic performance and flow field in the split-stream rushing muffler unit," *Journal of Sound and Vibration*, vol. 430, pp. 185–195, 2018.

[21] Y. Chang, M. Chiu, and S. Huang, "Numerical analysis of circular straight mufflers equipped with three chambers at high-order-modes," *Applied Acoustics*, vol. 155, pp. 167–179, 2019.

[22] W. Wang, Y. Zhou, Y. Li, and T. Hao, "Aerogels-filled Helmholtz resonators for enhanced low-frequency sound absorption," *The Journal of Supercritical Fluids*, vol. 150, pp. 103–111, 2019.

[23] M. Červenka and M. Bednařík, "Optimized compact wideband reactive silencers with annular resonators," *Journal of Sound and Vibration*, vol. 484, Article ID 115497, 2020.

[24] J. Fu, M. Xu, W. Zheng, Z. Zhang, and Y. He, "Effects of structural parameters on transmission loss of diesel engine muffler and analysis of prominent structural parameters," *Applied Acoustics*, vol. 173, Article ID 107686, 2021.

[25] C. Lu, W. Chen, Z. Liu, S. Du, and Y. Zhu, "Pilot study on compact wideband micro-perforated muffler with a serial-parallel coupling mode," *Applied Acoustics*, vol. 148, pp. 141–150, 2019.

[26] S. Chivate, P. Hujare, R. Askhedkar, D. Hujare, and S. Chinchanikar, "A review on acoustic performance analysis of reactive muffler," *Materials Today: Proceedings*, vol. 63, pp. 613–622, 2022.

[27] K. Ashok Reddy, "A critical review on acoustic methods & materials of a muffler," *Materials Today: Proceedings*, vol. 4, no. 8, pp. 7313–7334, 2017.

[28] F. Yiliang and J. Zhenlin, "Finite element predictive method and analysis for the acoustic attenuation performance of hybrid mufflers," *Acta Acustica*, vol. 47, no. 5, pp. 675–685, 2022.

[29] C. Zhixiang, J. Zhenlin, M. Qingzhen, C. Guoqiang, M. Xiangqi, and Z. Chao, "Transmission loss calculation and performance analysis of perforated-tube mufflers with non-uniform flow," *Technical Acoustics*, vol. 41, no. 5, pp. 705–710, 2022.

[30] H. Kangjian and J. Zhenlin, "Three-dimensional time-domain simulation and characteristic analysis of the nonlinear acoustic impedance of circular orifice," *Acta Acustica*, vol. 48, no. 2, pp. 373–382, 2023.

[31] Z. Yalin, J. Haojie, M. Jiangang, W. Lv, F. Qingchuan, and Z. Guoqing, "Calculation model of transmission loss for arrayed elements dissipative silencers," *Journal of Applied Acoustics*, vol. 2023, pp. 1–9, 2023.

[32] J. Fu, W. Zheng, M. Xu, W. Wang, and Y. Huang, "Study on the influence of structure factors of diesel engine exhaust purification muffler on transmission loss in different frequency bands," *Applied Acoustics*, vol. 180, Article ID 108147, 2021.

[33] B. Rong, *Analytical and experimental investigation on acoustic performance of hybrid muffler*, PHD Thesis, Hefei University of Technology, Hefei, China, 2012.